Self-assembling Gn head ferritin nanoparticle vaccine provides full protection from lethal challenge of Dabie Bandavirus in aged ferrets

Dokyun Kim[†1], Eunha Kim[†2,3,4], Semi Kim[2,3,4], Youseung Chung[5], Chih-Jen Lai[1], Inho Cha[1], Sung-Dong Cho[5], Yunseo Choi[5], Xinghong Dai[6], Stephanie Kim[1], Seokmin Kang[1], Mi-Jeong Kwak[1], Ziyi Liu[1], Younho Choi[7], Su-Hyung Park[5], Young Ki Choi[2,3,4#], Jae U. Jung[1#]

[1]Department of Cancer Biology, Infection Biology Program, and Global Center for Pathogen and Human Health Research, Lerner Research Institute, Cleveland Clinic, Cleveland, OH 44195, USA

[2]College of Medicine and Medical Research Institute, Chungbuk National University, Cheongju, Republic of Korea

[3]Zoonotic Infectious Disease Research Center, Chungbuk National University, Cheongju, Republic of Korea

[4]Center for Study of Emerging and Re-emerging Viruses, Korea Virus Research Institute, Institute for Basic Sciences, Daejeon, Republic of Korea

[5]Graduate School of Medical Science and Engineering, Korea Advanced Institute of Science and Technology, Daejeon, Republic of Korea

[6]Department of Physiology and Biophysics, Case Western Reserve University, Cleveland, OH 44106, USA

[7]Florida Research and Innovation Center, Cleveland Clinic, Port St. Lucie, FL, USA

Running title: Dabie Bandavirus Gn Head-Ferritin nanoparticle vaccine

#Correspondence: Address correspondence to
Jae U. Jung, jungj@ccf.org
Young Ki Choi, choiki55@chungbuk.ac.kr

†These authors contributed equally to this work. Author order was determined in order of contribution.

Abstract

Dabie Bandavirus (DBV), previously known as Severe Fever with Thrombocytopenia Syndrome (SFTS) Virus, induces a characteristic thrombocytopenia with a mortality rate ranging from 12% to as high as 30%. The sero-prevalence of DBV in healthy people is not significantly different among age groups, but clinically diagnosed SFTS patients are older than ~50 years, suggesting that age is the critical risk factor for SFTS morbidity and mortality. Accordingly, our immune-competent ferret model demonstrates an age (>4 years old)-dependent DBV infection and pathogenesis that fully recapitulates human clinical manifestation. To protect the aged population from DBV-induced SFTS, vaccine should carry robust immunogenicity with high safety profile. Previous studies have shown that glycoproteins Gn/Gc are the most effective antigens to induce both neutralizing antibody (NAb)- and T cell-mediated immunity for full protection from DBV infection. Here, we report the development of a protein subunit vaccine with 24-mer self-assembling ferritin (FT) nanoparticle to present the DBV Gn head region (GnH) to enhance immunogenicity. Anion exchange chromatography and size exclusion chromatography readily purified the GnH-FT nanoparticles to homogeneity with structural integrity. Mice immunized with GnH-FT nanoparticles induced robust NAb response and T-cell immunity against DBV Gn. Furthermore, aged ferrets immunized with GnH-FT nanoparticles were fully protected from DBV challenge without SFTS symptoms such as body weight loss, thrombocytopenia, leukopenia, and fatality. This study demonstrates that DBV GnH-FT nanoparticles provide an efficient vaccine efficacy in mouse and aged ferret models and should be an outstanding vaccine candidate targeted for the aged population against fatal DBV infection.

55 **Importance**

56 Dabie Bandavirus (DBV) is an emerging tick-borne virus that causes Severe Fever with
57 Thrombocytopenia Syndrome (SFTS) in infected patients. Human SFTS symptoms progress
58 from fever, fatigue, and muscle pain to the depletion of white blood cells and platelets with
59 fatality rates up to 30%. The recent spread of its vector tick to over 20 states in the United
60 States increases the potential for outbreaks of the SFTS beyond the East Asia. Thus, the
61 development of vaccine to control this rapidly emerging virus is a high priority.

62 In this study, we applied self-assembling ferritin (FT) nanoparticle to enhance the
63 immunogenicity of DBV Gn head domain (GnH) as a vaccine target. Mice immunized with the
64 GnH-FT nanoparticle vaccine induced potent antibody responses and cellular immunity.
65 Immunized aged ferrets were fully protected from the lethal challenge of DBV. Our study
66 describes the GnH-FT nanoparticle vaccine candidate that provides protective immunity against
67 the emerging DBV infection.

68

Introduction

Dabie Bandavirus (DBV), previously known as Severe Fever with Thrombocytopenia Syndrome (SFTS) Virus (SFTSV), is an emerging Bunyavirus responsible for causing SFTS in infected individuals (1). Since its initial identification in 2009 (2), the virus has established endemic infections in China, South Korea, and Japan, and has recently expanded to Southeast Asia (1, 3, 4). Prognoses of human DBV infection begin with flu-like symptoms, such as fever, fatigue, myalgia, and progress to hemorrhagic manifestations, including leukopenia, thrombocytopenia, and multiorgan failure, with fatality rates ranging from 12% to 30% (1, 5, 6). The severity of SFTS and its outcomes exhibit a clear age-dependence, as the vast majority of fatal cases and hospitalizations occur in individuals aged 50 or older (7, 8). However, no licensed vaccine or therapy against DBV is currently available. Consequently, the World Health Organization (WHO) and the United States National Institute of Allergy and Infectious Diseases (NIAID) have recently designated DBV as one of their priority pathogens (9) and Category C agents (10), respectively, representing emerging pathogens with outbreak potential. This designation aims to stimulate research interest in the development of vaccines and therapies for DBV.

DBV belongs to the *Bandavirus* genus within the *Phenuiviridae* family of the *Bunyavirales* order and carries a single-stranded, negative-sense genome divided into three segments: L, M, and S. The M segment encodes a precursor glycoprotein Gn/Gc, which is subsequently processed into Gn and Gc by host proteases (11). The Gn and Gc proteins assemble highly ordered capsomers as dimers on the viral surface. Gn is responsible for viral attachment to host cells through receptor binding, enabling Gc to mediate membrane fusion (12). Previous studies have identified DBV-neutralizing antibody epitopes on the head region of Gn (13-15), strongly suggesting the potential of DBV Gn as a vaccine candidate. Furthermore, our prior efforts to develop a DBV DNA vaccine demonstrated protection against lethal DBV challenge and the most potent induction of immunity when immunized with the M segment, which encodes the glycoproteins (16).

There has been limited success in developing vaccines against DBV due to the absence of an immunocompetent animal model that replicates clinical symptoms from human DBV infection and subsequent SFTS pathogenesis. In particular, the failure to reproduce age-dependent disease progression and clinical outcomes has been a significant obstacle in developing a vaccine to protect the most vulnerable group – the elderly population. We have recently presented an immunocompetent ferret model that highly replicates human DBV infection and clinical symptoms of SFTS. Aged ferrets (4 years or older) fully recapitulates SFTS

disease pathologies, characterized by fever, thrombocytopenia, leukopenia, and viremia in blood and organs, resulting in 93% fatality rate (17). Aged ferret model have been applied to DBV vaccine development using a live-attenuated vaccine with a mutation in its major virulence factor (non-structural protein, NSs) (18) and a DNA vaccine encoding the M segment to express Gn and Gc (16). Immunized aged ferrets developed strong humoral and cellular immunity and were fully protected from lethal DBV challenge.

The most vulnerable group to DBV infection and fatal SFTS is the elderly population, which experiences suboptimal induction of immunity and a high risk of vaccine-related adverse effects (19). Therefore, a vaccine development approach with an excellent safety profile and immunogenicity is required to effectively protect the elderly population against DBV infections. Protein subunit vaccines of viral antigens containing neutralization epitopes have been suggested as safe vaccine candidates; however, host immune system often fails to effectively react against soluble antigens due to their small sizes (20). Fortunately, recent advances nanotechnology and molecular biology have transcended previous limitations by employing nanoparticle engineering as a toolkit for vaccine development (21). The immunogenicity of nanoparticle-engineered vaccines has surpassed that of traditional protein subunit vaccines. Moreover, recent research has elucidated the immunological mechanisms behind the enhanced immunogenicity: higher activation and formation of germinal centers (22), improved antigen transport to draining lymph nodes (23), and antigen presentation by follicular dendritic cells and helper T cells (24). Among the naturally derived and artificially designed nanoparticles, ferritin is the most extensively studied and applied nanoparticle. Found across life's kingdoms, ferritin possesses a conserved function in storing excess iron (Fe^{2+}) inside the nanoparticle to quench the Fenton reaction, which generates reactive oxygen species that cause cellular damage. More importantly, ferritin forms a higher-order homopolymer structure of the self-assembly of 24 ferritin monomer subunits, facilitating expression and purification for application in biotechnology. Its molecular amenability via fusion peptides from recombinant DNA constructs has enabled further application of the self-assembling nanoparticle to vaccine development (25).

One of the most applied ferritins is hybrid ferritin, engineered by fusing the *Helicobacter pylori* ferritin backbone with NH_2-terminal tail from bullfrog (*Rana catesbeiana*) ferritin lower subunit. The NH_2-terminal tail forms radial projections on the threefold-axis points of the self-assembled nanoparticle, efficiently presenting viral immunogens fused in the recombinant DNA construct to provide stronger protective immunity at significantly lower doses than soluble antigens (26, 27). Due to the low amino acid sequence similarity of *H. pylori* and bullfrog ferritin to human ferritin, the hybrid ferritin has minimal risk of vaccine-related adverse effects or

137 autoimmunity from antigen mimicry. Consequently, the hybrid nanoparticle has been widely
138 applied as an effective immunogen carrier platform in diverse vaccine developments, including
139 MERS-CoV (28), SARS-CoV-2 (25), Influenza (27), and Epstein-Barr Virus (26). These indicate
140 the utility of ferritin nanoparticles as an outstanding vaccine carrier platform to induce strong
141 protective immunity against infectious agents.

142 In this paper, we demonstrate the immunogenicity of the self-assembling DBV Gn Head
143 (GnH)-ferritin (GnH-FT) nanoparticle as an effective DBV vaccine candidate. We purified GnH-
144 FT nanoparticles from transfected HEK293T cells, characterized their biochemical, antigenic,
145 and structural profiles, and immunized mice and aged ferrets to investigate the induction of
146 humoral and cellular immunity. Furthermore, we challenged vaccinated aged ferrets with a lethal
147 dose of DBV and observed protective immunity against DBV. These data suggest the DBV
148 GnH-FT nanoparticle as a promising vaccine candidate, providing protective immunity against
149 DBV infection and subsequent SFTS pathogenesis.
150

151 **Results**

152 **Molecular design, purification, and characterization of DBV GnH-ferritin nanoparticles**

153 A majority of DBV-neutralizing antibodies from human convalescent sera target the head
154 region of Gn (13, 14), which mediates viral attachment to host cells. Furthermore, our recent
155 study of DBV DNA vaccine has identified the viral glycoproteins as the most immunogenic
156 antigen among the viral proteins. The DBV Gn head (GnH) gene was first human-codon-
157 optimized and fused to the IL-2 signal peptide at the N-terminus and the *H. pylori*-bullfrog hybrid
158 ferritin at the C-terminus to generate GnH-ferritin (GnH-FT) (Fig. 1A). HEK293T cells were
159 transfected with GnH-FT expression plasmid or the hybrid ferritin (FT) with the signal peptide,
160 and the cell supernatants were collected to purify the GnH-FT and FT nanoparticles by anion
161 exchange chromatography and size exclusion chromatography.

162 The purified FT (Fig. 1B) and GnH-FT (Fig. 1C) nanoparticles were homogenous, as
163 demonstrated by size exclusion chromatography with specific columns exhibiting maximal
164 separating resolution at several hundred kilodaltons and a few megadaltons, respectively.
165 Additionally, the chromatograms of GnH-FT and FT nanoparticles showed peaks at fractions
166 corresponding to the expected molecular weight as 24-mer nanoparticles. We further tested if
167 the purified FT and GnH-FT nanoparticles retained the 24-mer nanoparticle structures by
168 loading the purified fractions onto SDS-PAGE without boiling ("NB" for not boiled) or with boiling
169 ("B" for boiled). The purified nanoparticles retained the higher-order structure without boiling but
170 disassembled into subunit monomers upon boiling (Fig. 1D, 1E). As a result, bands appeared at
171 the expected molecular weights of monomers calculated based on previously solved GnH
172 structures (15). Immunoblotting analysis of different fractions (marked with colored arrows) of
173 size exclusion chromatography with anti-DBV Gn antibody also confirmed the presence of GnH-
174 ferritin with intensities matching the peak heights of size exclusion chromatogram (Fig. 1F).
175 These results indicate that the purified GnH-FT nanoparticles retain the higher-order structure
176 from self-assembly.

177

178 **Purified GnH-FT nanoparticle retains the higher-order structure and presents GnH on its**
179 **surface**

180 According to computer-assisted modeling based on previous reports using ferritin
181 nanoparticles as carrier platforms, the GnH antigen was expected to radially project from three-
182 fold axis points of the nanoparticle (Fig. 2A, 2B). Negative staining transmission electron
183 microscopy (EM) and cryo-EM of FT nanoparticles demonstrated a homogenously smooth
184 circular surface with an average diameter of 9.5nm (Fig. 2C, Fig. S1A), while those of GnH-FT

185 nanoparticles showed clearly visible protrusions from the ferritin core with an average diameter
186 of 14.7nm (Fig. 2D and Fig. S1B). These protrusions appeared as an extra layer of white,
187 smeared halo surrounding the ferritin core in the cryo-EM 2D class averages of GnH-FT
188 nanoparticles (Fig. 2F) compared to those of the FT nanoparticles (Fig. 2E). These data
189 indicated that the GnH was flexible on the surface of the ferritin particle, and its presence did not
190 affect the assembly of the ferritin particle.
191
192 **Immunization with GnH-FT nanoparticle induces humoral immunity and cellular immunity**
193 ***in vivo***
194 To enhance the relatively weaker immunogenicity of protein subunit vaccines, a diverse
195 selection of adjuvants is administered in combination with protein vaccine candidate. One of the
196 safest among the variety of adjuvants is MF59, an oil-in-water emulsion adjuvant used in
197 adjuvanted flu vaccines (29-32). We combined the veterinary equivalent MF59, AddaVax, with
198 FT or GnH-FT nanoparticles for immunization. 8-10-week-old BALB/c mice (n=6 per antigen)
199 were immunized with a total of 3 doses at 3-week intervals of 3.3μg of FT nanoparticle –
200 equimolar to 10μg of GnH-FT nanoparticle – or 1μg, 5μg, or 10μg of GnH-FT nanoparticle via
201 the intramuscular route. Blood was drawn prior to immunization (week 0) and every week
202 starting 2 weeks after the priming immunization. Total IgG antibody against GnH soluble protein
203 reached a maximal level at 2 weeks after the 2nd dose of immunization (first booster) and did not
204 further increase upon the 3rd dose (second booster) among all three doses of GnH-FT
205 nanoparticle immunization (Fig. 3B). Interestingly, there was no statistically significant difference
206 in the induction of total anti-GnH IgG levels across different doses of GnH-FT nanoparticle,
207 indicating that 1μg GnH-FT dose was sufficient for inducing strong antibody response.
208 We performed a neutralization assay using replication-defective recombinant Vesicular
209 Stomatitis Virus (rVSV) carrying DBV glycoproteins, Gn and Gc, and luciferase reporter gene
210 (rVSV-DBV G). Unlike total anti-GnH antibody response that reached a maximal level after the
211 2nd immunization, neutralizing antibody (NAb) titer continuously increased over the 3
212 immunizations with GnH-FT nanoparticle (Fig. 3C). Immunization with 1μg GnH-FT nanoparticle
213 elicited the most robust neutralizing antibody response against DBV, followed by 5μg and 10μg.
214 Consistently with the total IgG, there was no significant induction of NAb against DBV upon
215 immunization with FT nanoparticle alone (Fig. 3C). These data suggest that 1μg GnH-FT may
216 be an optimal dose for 3-dose regimen to elicit strong NAb response against DBV infection.
217 Although NAb titer is a critical marker of vaccine efficacy, many studies have shown the
218 importance of cellular immunity for antiviral immunity (33, 34). To perform IFN-γ ELISpot,

219 spleens from immunized mice at week 8 (two weeks after the 3rd immunization) were harvested,
220 *ex vivo* stimulated with a pool of overlapping peptides (OLPs) spanning GnH, and subsequently
221 subjected to IFN-γ ELISpot. This showed that IFN-γ secretion was induced across all doses of
222 GnH-FT nanoparticle immunization, whereas immunization with 1μg GnH-FT nanoparticle
223 elicited the most robust IFN-γ secretion (Fig. 3D). In addition, GnH-FT nanoparticle
224 immunization successfully induced TNF-α and IL-2 production from OLP-stimulated CD4+ T
225 cells, whereas FT-nanoparticle immunization did not induce those cytokine productions (Fig. 3E).
226 Finally, there was no significant production of TNF-α and IL-2 from OLP-stimulated CD8+ T cells
227 (data not shown). These showed that the maximal induction of NAb, IFN-γ, TNF-α and IL-2 were
228 observed from 1μg dose of GnH-FT nanoparticle immunization. These data corresponded to the
229 previous reports of robust activation of protective immunity from the low dose immunization of
230 nanoparticle vaccines (25-27) and Adenoviral vector vaccine (35). Collectively, these results
231 demonstrate that the immunization of DBV GnH-FT nanoparticle effectively elicits both NAb
232 production and T-cell response in mice.
233
234 **Aged ferret immunized with GnH-FT nanoparticle form antibody responses against DBV**
235 Naïve 4-year-old ferrets (n=12 ferrets per antigen) were vaccinated via intramuscular
236 injection with FT or GnH-FT nanoparticles with AddaVax adjuvant for a total of 3 immunizations
237 at 2-week intervals. Blood of immunized ferrets was collected on the day of immunization to
238 characterize antibody responses (Fig. 4A). While total anti-GnH IgG titers were dramatically
239 increased after the 1st or 2nd vaccination, they were further escalated after the 3rd vaccination,
240 suggesting that the vaccination protocol of total 3 doses maximizes the antibody response in
241 aged ferret. We did not observe significant increase of IgG level upon booster immunizations,
242 which might be due to the potential saturation of our assay (Fig. 4B). Consistently, serum NAb
243 titers against DBV CB1/2014 strain were continuously increased following the priming
244 vaccination and subsequent booster vaccinations (Fig. 4C). On the contrary, neither anti-GnH
245 antibody nor anti-DBV NAb was detected from control ferrets immunized with FT nanoparticles.
246 These data indicate that the GnH-FT nanoparticle effectively induces antibody responses
247 against DBV in aged ferret model.
248
249 **Immunization with GnH-FT nanoparticle provides full protection against lethal DBV**
250 **challenge in aged ferrets**
251 To evaluate the protective efficacy of GnH-FT vaccines, FT or GnH-FT vaccinated aged
252 ferrets were intramuscularly challenged with a lethal dose of DBV CB1/2014 strain ($10^{7.6}$ $TCID_{50}$)

253 in 2 weeks after the third vaccination, and monitored for clinical signs of infection, viral titers and
254 platelet counts in the blood, body weight, body temperature, and survival rate for the following
255 14 days, with evaluations every other day. Blood was collected every other day to measure
256 platelet and white blood cell counts to observe thrombocytopenia and leukopenia (Fig. 4A).
257 Strikingly, all ferrets immunized with GnH-FT nanoparticles were fully protected from
258 lethal DBV challenge, while ferrets immunized with FT nanoparticles suffered significant body
259 weight loss up to 20% and succumbed to death (Fig. 5A and 5B). Aged ferrets immunized with
260 GnH-FT nanoparticles showed minimal increases in body temperature, while those immunized
261 with FT nanoparticles experienced severe fever (Fig. 5C). Platelet and white blood cell counts
262 were also measured from the blood samples to test for the characteristic symptoms of
263 thrombocytopenia and leukopenia. Consistent with body weight, temperature, and survival,
264 aged ferrets immunized with GnH-FT nanoparticles showed little or no significant reduction in
265 platelet and white blood cell counts (Fig. 5D). In contrast, aged ferrets immunized with FT
266 nanoparticles demonstrated dramatic reductions in both platelet and white blood cell counts
267 before the fatal outcome (Fig. 5E).
268 To assess viral burden in multiple organs upon lethal DBV challenge, we sacrificed 3
269 ferrets at days 2, 4, and 6 post-infection and harvested serum, spleen, liver, and kidney. Viral
270 titers were measured as RNA copy numbers using real-time PCR. Aged ferrets immunized with
271 FT-nanoparticle demonstrated significant viremia in liver and kidney upon lethal DBV challenge
272 and succumbed to the viral challenge (Fig. 6C and 6D). However, aged ferrets immunized with
273 GnH-FT nanoparticles rapidly cleared the challenging virus so that the viral titer quickly
274 decreased to the limit of detection or lower (Fig. 6C and 6D). These data indicate that
275 immunization with GnH-FT nanoparticles provides complete protection against SFTS
276 pathogenesis upon lethal DBV challenge and promotes viral clearance in aged ferrets.
277

Discussion

DBV, previously named SFTSV, is an emerging pathogen causing fatal SFTS in infected patients. Since its original discovery in China, it has established endemic infection in South Korea, Japan, and China, and spread to Southeast Asian countries (3, 4, 8). A clear age-dependence in pathogenesis from human DBV infection is evident, as the majority of hospitalization cases and almost all fatal infections occur in age groups of 50 or above (7). The vector tick – *Haemaphysalis longicornis* – used to have a relatively confined habitat in East Asia. However, its parthenogenetic reproduction has enabled recent rapid spread to other continents, including Australia and North America (36, 37). Combined with the spread of the tick, there have been growing concerns of a DBV outbreak beyond East Asia (1, 7, 37, 38). Here, we demonstrate the immunogenicity of the self-assembling GnH-FT nanoparticle as an effective DBV vaccine candidate. Mice immunized with the FT nanoparticle vaccine induced potent antibody responses and cellular immunity. Immunized aged ferrets were fully protected from the lethal infection of DBV. Our results strongly demonstrate the DBV GnH-FT nanoparticle as a promising vaccine candidate, providing protective immunity against DBV infection and subsequent SFTS pathogenesis.

Among DBV viral proteins, Gn and Gc glycoproteins are initially translated as a precursor glycoprotein from the M segment of the viral genome and subsequently processed into separate proteins by host protease (11). Structural analyses of closely related Bunyaviruses – Heartland Bandavirus (HRTV) and Rift Valley Fever Virus (RVFV) – have identified that Gn and Gc form heterodimers and create higher-order structures on the viral surface (39, 40). Gn and Gc contribute to viral infection with Gn attaching to the host cell membrane and Gc mediating membrane fusion for endocytosis (12, 41). Our previous study demonstrated that the most potent immunogenicity was observed upon immunization of the Gn/Gc-containing M segment DNA in mice and aged ferrets (16). Furthermore, all neutralizing antibodies reported to date from convalescent human sera have mapped their epitopes on the head region of Gn (13-15), strongly suggesting its potential as a prime target for vaccine development.

Previous studies have demonstrated higher immunogenicity at lower doses of nanoparticle vaccines compared to conventional protein vaccines while retaining the advantage of reduced reactogenicity (26, 27). To develop a safe yet sufficiently immunogenic vaccine for aged population with weakened immunity, we formulated GnH-FT nanoparticle with an adjuvant with an established safety profile in the elderly population. Purified GnH-FT nanoparticles showed their integrity in presenting the DBV GnH on the carrier nanoparticle. Mice and aged ferrets immunized with GnH-FT nanoparticle robustly induced DBV-recognizing IgG and NAb.

312 While NAb titers increased over booster immunizations, the highest NAb titers were observed
313 from the immunization with 1μg of GnH-FT nanoparticle. Mice immunized with 1μg GnH-FT
314 nanoparticle also showed the strongest T cell response. This corresponds to the previous
315 findings that immunizations with low doses of ferritin-fused nanoparticle provide protective
316 immunity against Influenza virus (0.22μg) (27), Epstein-Barr virus (0.5μg) (26) and SARS-CoV-2
317 vaccine (15μg) (25). Similar results have been recently reported in a large clinical trial
318 investigating the immunogenicity of Adenoviral vector (Ad26.COV2.S)-based vaccine against
319 SARS-CoV-2. Immunization with a lower dose (5E10) of Ad26.COV2.S particles induced more
320 potent immunity with milder side effects than a higher dose (1E11) of Ad26.COV2.S particles
321 (35). These studies further support the strong immunogenicity of ferritin nanoparticle at low
322 doses as vaccine carrier. From our mouse *in vivo* studies, immunization with 1μg GnH-FT
323 provided the most robust induction of NAbs and T-cell responses. Because dose is closely
324 related to vaccine-related adverse effects, additional studies are needed to optimize GnH-FT
325 immunization protocols to enhance vaccine-mediated immunity while minimizing reactogenicity.
326 Specifically, since our goal is to develop a safe yet sufficiently immunogenic vaccine for aged
327 population with weakened immunity, we will further investigate the immunological mechanism
328 behind the low dose of GnH-FT nanoparticle to induce potent vaccine immunity.
329 There are six genotypes of DBV (A to F) reported to date from South Korea, Japan, and
330 China (7). Geographical locations with endemic DBV infection display varying abundances of
331 these genotypes and, therefore, varying fatality rate. The GnH is encoded by the M segment of
332 the DBV genome, which exhibits lower than 10% viral nucleotide variation (42, 43) and 6%
333 amino acid variation (44), although the numbers vary across genotypes. Another study reported
334 broad cross-reactivity of the HB29 strain of DBV (used in this study) with both autologous and
335 heterologous genotypes of DBV (16, 45). Our previous DBV vaccine development also reported
336 cross-protection of live-attenuated vaccines using HB29 (16, 46). This suggests that HB29 may
337 serve as an optimal standard strain for DBV vaccine development. Protective immunity can be
338 expanded even further for broader protection by exchanging the GnH on the FT nanoparticle
339 with the GnH of other genotypes as “plug and play” platform. Future studies on immunity against
340 other genotypes will provide insights into the potential for broad protection by GnH-FT
341 immunization.
342 FT nanoparticles have been widely applied in biotechnology due to its well understood
343 assembly process, wide application as carrier, and thermal and chemical stability. These
344 advantages facilitate manufacture, storage, and transportation of FT nanoparticle vaccines.
345 Further characterizations of the maintenance of GnH-FT nanoparticle stability will streamline

346 logistics aspects of the vaccine candidate and contribute to developing an effective and
347 accessible vaccine against DBV.

348 In conclusion, we designed and purified DBV GnH-FT nanoparticle presenting GnH
349 while retaining the structural integrity of nanoparticles and antigenicity of GnH. Furthermore, we
350 evaluated its immunological efficacy as a vaccine candidate in mouse and aged ferret models.
351 Immunized mice with GnH-FT nanoparticle induced strong humoral immunity and cellular
352 immunity. Immunized aged ferrets showed not only effective induction of total IgG antibody and
353 NAb but also full protection from SFTS symptoms and fatality upon lethal DBV challenge.
354 Although previous reports have shown strong efficacies of live attenuated virus vaccines (46)
355 and DNA vaccine (16), these approaches still have safety concerns, especially in elderly
356 population. Our protein subunit FT nanoparticle vaccine that has prospective safety profile
357 demonstrates outstanding protection efficacy in mouse and aged ferret models. This suggests
358 the GnH-FT nanoparticle as a potential safe vaccine targeted for the elderly population that is a
359 prime target of DBV infection and subsequent SFTS.

360 **Material and Methods**

361 **Expression and purification of the nanoparticles**

362 Expression vectors to purify the nanoparticles were prepared as previously described in
363 our earlier publication (25). Dabie Bandavirus (DBV) glycoprotein Gn gene (GenBank
364 NC_018138.1) was codon-optimized for human codon usage (Genscript) and cloned into the
365 expression vector. At 70% confluency, HEK293T cells (ATCC) cells had their media changed to
366 FreeStyle 293 medium (Gibco) and transfected with the plasmids. Supernatants were
367 concentrated with 100kDa or 500kDa MWCO filters on Labscale TFF (Sigma). Concentrated
368 supernatants were flowed into anion Resource Q column (Cytiva) for anion exchange
369 chromatography on NGC FPLC (Bio-Rad) running with pH8.0, 20mM Tris-Cl and a gradient
370 increase from 0M to 1M NaCl at 3.0ml/min. Fractions from NaCl concentration of 200mM to
371 500mM were collected and further purified by size exclusion chromatography. NGC FPLC
372 equipped with Superdex 200 Increase 10/300 GL (for FT nanoparticle) and Superose 6 Increase
373 10/300 GL (for GnH-FT nanoparticle) columns (Cytiva) were used with PBS at 0.1ml/min.
374 Collected fractions were analyzed by loading onto SDS-PAGE with or without boiling for 10min
375 at 95°C and stained with Coomassie Brilliant blue. Western blot of the fractions was performed
376 using in house-generated mouse monoclonal antibody against DBV Gn.

377 To purify DBV GnH-10His protein, HEK293T cells were transfected with the mammalian
378 expression vector under the same condition as for nanoparticle purification. Supernatant was
379 flowed into HisTrap HP column (Cytiva) using NGC at flow rate of 5ml/min and eluted by
380 gradient increase of imidazole from 0mM to 500mM in 150mM NaCl and 20mM Tris-Cl, pH8.0.
381 Fractions were tested for yield and purity by SDS-PAGE and stored at -80°C in 10% glycerol.

382

383 **Computer-assisted 3D modeling of FT and GnH-FT nanoparticles**

384 Hypothetical structures of FT nanoparticle and GnH-FT nanoparticles were designed
385 based on previously solved DBV Gn (PDB: 5Y11) and *H. pylori*-bullfrog hybrid ferritin (PDB:
386 3EGM) with Chimera (University of California San Francisco), PyMol (Schroedinger), and
387 Meshmixer (Autodesk). The model was revised to take account for the size ratio of FT
388 nanoparticles and GnH-FT nanoparticles.

389

390 **Transmission electron microscopy and cryo-EM analysis of FT and GnH-FT**
391 **nanoparticles**

392 For negative staining transmission electron microscopy (EM), carbon-coated grids were
393 rendered hydrophilic by glow-discharge and applied with a drop of purified nanoparticles in

394 DPBS. After absorption for 1min, excess sample was blotted away, and the grids were stained
395 with 1% (w/v) uranyl acetate. After drying, the grids were imaged on a Talos F200X G2
396 microscope at 200kV.
397 To prepare cryo-EM grid, an aliquot of 3.5μL purified nanoparticles at ~1mg/mL
398 concentration was applied to a 300-mesh Quantifoil R1.2/1.3 Cu grid pre-treated with glow-
399 discharge, blotted in a Vitrobot Mark IV machine (force -5, time 3 s), and plunge-frozen in liquid
400 ethane. The grid was loaded in a Titan Krios microscope equipped with Gatan BioQuantum K3
401 imaging filter and camera. A 20-eV slit was used for the filter. Data collection was done with
402 serialEM (47). Images were recorded at 81,000× magnification, corresponding to a pixel size of
403 1.06 Å/pix. A defocus range of -1.0μm to -1.8μm was set. A total dose of 50 e-/Å2 of each
404 exposure was fractionated into 50 frames. The first two frames of the movie stacks were not
405 included in motion-correction. CryoEM data processing was performed on the fly with
406 cryoSPARC Live (48) following regular single particle procedures.
407
408 **Virus propagation and titration**
409 Methods from our previous publications were applied for DBV propagation and titration
410 (16, 17). Briefly, Vero E6 (ATCC, CRL-1586) cells were cultured at 37°C and 5% CO_2 with
411 Dulbecco's modified Eagle's medium (DMEM) supplemented with 10% FBS. Cells were infected
412 with CB1/2014 strain of DBV at confluency and supernatant was collected 7days later. The
413 supernatant was centrifuged to remove cell debris and stored at -80°C until further use. Viral
414 titer in form of $TCID_{50}$ was determined by immunofluorescence assay (IFA) using in house-
415 generated mouse monoclonal antibody recognizing DBV nucleoprotein (Np).
416
417 **Animal Care**
418 BALB/c mice at ages of 6-8 weeks (Jackson Laboratories, Maine) were housed in
419 Biological Resource Unit facility within Lerner Research Institute, Cleveland Clinic, with 12h
420 light/dark cycle with access to water and diet.
421 Aged ferrets at ages of 48-50 months (ID Bio, Cheongju, South Korea) were housed in
422 Laboratory Animal Research Center of Chungbuk National University (LARC) (Cheongju, South
423 Korea) with 12h light/dark cycle with access to water and diet. All mouse and ferret cares were
424 performed in accordance with the institutional animal care guideline and experiment protocols
425 approved by Institutional Biosafety Committee (IBC) and Institutional Animal Care and Use
426 Committee (IACUC) in Cleveland Clinic and Chungbuk National University, respectively. After
427 viral challenge, the animals were monitored more frequently by the authors or veterinary

428 technicians on duty. Viruses were handled in an enhanced biosafety level 3 containment
429 laboratory as approved by the Korean Centers for Disease Control and Prevention (KCDC-14-3-
430 07).
431
432 **Animal immunization and sample collection**
433 Mice were intramuscularly immunized with 3.3μg of FT nanoparticles, or 1μg, 5μg, or
434 10μg of GnH-FT nanoparticles in hind leg. The antigens were prepared in 50μl of DPBS and
435 mixed with 50μl AddaVax adjuvant (veterinary equivalent to MF59, Invivogen). Blood was
436 collected from saphenous vein or retro orbital sinus to titer neutralizing antibodies.
437 For ferret immunization, 15μg FT nanoparticles or GnH-FT nanoparticles in 300μl was
438 mixed with 300μl of AddaVax adjuvant for intramuscular immunization into the legs under
439 anesthesia. Blood was also collected at the anesthesia. Subsequently, ferrets were
440 intramuscularly infected with $10^{7.6}$ $TCID_{50}$/mL of DBV, which has shown 100% fatality in our
441 previous study (46). Their body weight and temperature were measured, and veterinary clinical
442 symptoms were observed. Blood was collected for hematological analysis every other day until
443 14 days post infection. Three animals per group were sacrificed at days 2, 4, and 6 to collect
444 serum, spleen, liver, and kidney with individual scissors to avoid cross-contamination.
445
446 **Titration of DBV Gn-recognizing antibodies and DBV-neutralizing antibodies in serum**
447 To measure total mouse IgG against GnH, FT and GnH-FT, ELISA plates (MaxiSorp,
448 ThermoFisher) were coated with respective antigens at concentration of 0.1μg/well. The plates
449 were blocked with 5% skim milk in 0.05% PBS-Tween 20. Heat-inactivated sera was diluted in
450 10-fold dilution series in DPBS and 100μl of the dilutions were incubated in the wells overnight
451 at 4°C. Plates were washed and incubated with HRP-conjugated anti-mouse IgG antibody
452 (Jackson Immunoresearch). For detection of antibodies, the plates were overlaid with TMB
453 substrate (ThermoFisher) and 1M sulfuric acid.
454 To measure mouse neutralizing antibody titer against DBV, we performed pseudovirus
455 neutralization assay as described in our previous publication (41). In brief, we co-incubated
456 serially 2-fold diluted sera with recombinant VSV carrying DBV glycoproteins and reporter
457 luciferase gene (rVSV-DBV-Luc). The inoculum was added to HEK293T cells and incubated at
458 37°C with 5% CO_2 and the luciferase signal was with analyzed using luciferase assay kit
459 (Promega).
460 For titration of total ferret IgG and neutralizing antibodies against DBV, we performed
461 ELISA and serum neutralization titration as previously described (16, 46). To titer total ferret IgG

462 titer, ELISA plates coated with antigen and blocked in same method as from mouse IgG titer.
463 Ferret sera were diluted in 2% skim milk in 0.05% PBS-Tween 20 from 1:50 to 1:50,000. 100μl
464 of diluted ferret sera were incubated in ELISA plates for 2h at room temperature. Plates were
465 then washed and incubated with HRP-conjugated anti-ferret IgG (KPL, South Korea). O-
466 phenylenediamine dihydrochloride substrate was added to develop color and 1M sulfuric acid
467 stop solution was added. After washing ELISA plates coated with GnH, the plates were blocked
468 and incubated with HRP-conjugated anti-ferret IgG (KPL, South Korea). O-phenylenediamine
469 dihydrochloride (ThermoFisher) was added to the plates and 1M sulfuric acid was added to stop
470 color development. OD values at 450nm were measured with a plate reader (iMark Microplate
471 reader, Bio-Rad).
472 Serum neutralization titer was measured as previously described (49). Briefly, heat-
473 inactivated serum samples were serially twofold diluted from a 1:2 to 1:128. Then, 50μl of the
474 diluted serum were mixed with equal volume of 200 focus-forming units of DBV for 1h at 37°C.
475 The mixture was adsorbed onto confluent Vero E6 cells in 96-well plate at 37°C for 1h. Media
476 was changed to maintenance medium and cells were maintained in incubator for 5 days. Cells
477 were then fixed with 10% formalin and stained with in house-generated anti-DBV Np antibody.
478 For $FRNT_{50}$, the cells were also stained with HRP-conjugated anti-mouse IgG antibody. Serum
479 neutralizing antibody titer was presented as reciprocal of the highest serum dilution neutralizing
480 fluorescence signal of DBV Np.
481
482 **Profiling T-cell immunity by IFN-γ ELISpot**
483 We referred to our previous publication (16). In brief, Multiscreen 96-well plates with
484 PVDF membrane (Milipore) were coated with 100ul of anti-mouse IFN-γ antibody (clone AN-18,
485 eBioscience, South Korea) overnight at 4°C. Mouse splenocytes were stimulated *ex vivo* with
486 overlapping peptide pool (OLP) of 78 of 15-mer peptides covering DBV GnH formulated at
487 0.625μg/ml for each peptide in RPMI medium (Gibco) in the 96-well plate. PMA at 10ng/ml and
488 ionomycin at 500ng/ml were included as positive controls and 0.5% DMSO was included as
489 negative control for stimulation. After 24h stimulation in 5% CO_2, 37°C incubator, plates were
490 washed to remove cells and incubated with 100μl of biotinylated anti-mouse IFN-γ antibody for
491 1h at RT, followed by wash and incubation with 100μL of streptavidin-alkaline phosphatase
492 (Invitrogen) for 1h at RT. 100ul of BCIP/NBT was added for 10min incubation at RT. Number of
493 spot forming units (SFUs) per cells were presented after subtracting SFUs from negative control
494 wells stimulated with 0.5% final concentration of DMSO.
495

496 **Intracellular cytokine staining**

497 Based our protocol from previous publication (16), we resuspended the splenocytes from
498 the immunized in 100μl of RPMI-1640 media. The cells were *ex vivo* stimulated with anti-
499 CD107a antibody (BD Biosciences, 553792), anti-CD28/CD49d antibody (BD Biosciences,
500 347690) and OLP or DMSO in 100μl. The mixture was incubated in 5% CO_2, 37°C incubator for
501 1hour and treated with 4μl of mixture of the complete RPMI-1640 media: Brefeldin A (GolgiPlug,
502 BD Biosciences, 555029):Monensin (GolgiStop, BD Biosciences, 554715) in 55:3:2. After
503 12hours of incubation in 5% CO_2, 37°C, the cells were washed with PBS and stained with
504 surface antibodies (anti-CD44 BV421 [BD Biosciences, 536970], anti-CD8a BV510 [BD
505 Biosciences, 563068], anti-CD62L BV650 [BD Biosciences, 564108], anti-CD3 BV786 [BD
506 Biosciences, 564010], anti-CD4 PerCP-Cy5.5 [BD Biosciences, 561115], and anti-CD19 APC
507 [BD Biosciences, 561738]) for 15 minutes at RT and washed. Cells were then fixed with 4%
508 paraformaldehyde in PBS and permeabilized. We then washed the cells and stained with FACS
509 antibodies (anti-IL-2 FITC [BD Biosciences, 562040], anti-TNF PE [BD Biosciences, 554419],
510 anti-IFN-γ [BD Biosciences, 557735], and anti-CD107a [BD Biosciences, 560647]) by 20
511 minutes of incubation at room temperature, washed twice with the permeabilization buffer and
512 resuspended with 300μl of PBS.

513

514 **Hematological analysis and viral titration from challenged ferrets**

515 We analyzed for hematological profile and tittered viremia as previously described (17).
516 Total white blood cell and platelet counts in whole ferret blood samples were analyzed using the
517 Celltac hematology analyzer (MEK-6550J/K, Nihon Kohden, Japan). Total RNA was extracted
518 with TRIzol reagent (ThermoFisher) and reverse-transcribed to generate cDNA using
519 QuantiTect Reverse Transcription system (Qiagen). Primers for real-time RT PCR (F:
520 AATTCACATTTGAGGGTAGTT), R: TATCCAAGGAGGATGACAATAAT) were designed to
521 recognize M segment of DBV genome. Real-time PCR was performed with SYBR Green
522 supermix and CFX Real-Time PCR detection system (Bio-Rad). Copy numbers were
523 normalized to GAPDH gene.

524

525 **Acknowledgments**

526 *H. pylori*-bullfrog ferritin construct was kindly provided by Drs. Jeffrey Cohen and Gary Nabel at
527 Vaccine Research Center, NIAID. This work was supported by National research foundation of
528 Korea (NRF-2020R1A5A2017476, 2020R1A2C3008339), Institute for Basic Science (IBS) of
529 Korea (IBS-R801-D1 to Y.K.C.), and National Institute of Health (CA251275, AI140705,

AI140718, AI152190, AI171201, AI172252, AI171443, DE023926, and DE028521) and Korea Research Institute of Bioscience and Biotechnology KGM9942011 (J.U.J.). We appreciate Carolyn Marks (Core Center of Excellence in Nano Imaging, University of Southern California) for technical assistance with transmission electron microscopy of nanoparticles.

Competing Financial Interests

Patent application is filed via Cleveland Clinic Foundation Innovations Office.

537 **References**

538 1. Casel MA, Park SJ, Choi YK. 2021. Severe fever with thrombocytopenia syndrome virus:
539 emerging novel phlebovirus and their control strategy. Experimental & Molecular Medicine
540 53:713-722.
541 2. Yu XJ, Liang MF, Zhang SY, Liu Y, Li JD, Sun YL, Zhang L, Zhang QF, Popov VL, Li C, Qu J, Li Q,
542 Zhang YP, Hai R, Wu W, Wang Q, Zhan FX, Wang XJ, Kan B, Wang SW, Wan KL, Jing HQ, Lu JX, Yin
543 WW, Zhou H, Guan XH, Liu JF, Bi ZQ, Liu GH, Ren J, Wang H, Zhao Z, Song JD, He JR, Wan T,
544 Zhang JS, Fu XP, Sun LN, Dong XP, Feng ZJ, Yang WZ, Hong T, Zhang Y, Walker DH, Wang Y, Li DX.
545 2011. Fever with thrombocytopenia associated with a novel bunyavirus in China. N Engl J Med
546 364:1523-32.
547 3. Rattanakomol P, Khongwichit S, Linsuwanon P, Lee KH, Vongpunsawad S, Poovorawan Y. 2022.
548 Severe Fever with Thrombocytopenia Syndrome Virus Infection, Thailand, 2019-2020. Emerg
549 Infect Dis 28:2572-2574.
550 4. Tran XC, Yun Y, Van An L, Kim SH, Thao NTP, Man PKC, Yoo JR, Heo ST, Cho NH, Lee KH. 2019.
551 Endemic Severe Fever with Thrombocytopenia Syndrome, Vietnam. Emerg Infect Dis 25:1029-
552 1031.
553 5. Jiang XL, Zhang S, Jiang M, Bi ZQ, Liang MF, Ding SJ, Wang SW, Liu JY, Zhou SQ, Zhang XM, Li DX,
554 Xu AQ. 2015. A cluster of person-to-person transmission cases caused by SFTS virus in Penglai,
555 China. Clin Microbiol Infect 21:274-9.
556 6. Zhang YZ, He YW, Dai YA, Xiong Y, Zheng H, Zhou DJ, Li J, Sun Q, Luo XL, Cheng YL, Qin XC, Tian
557 JH, Chen XP, Yu B, Jin D, Guo WP, Li W, Wang W, Peng JS, Zhang GB, Zhang S, Chen XM, Wang Y,
558 Li MH, Li Z, Lu S, Ye C, de Jong MD, Xu J. 2012. Hemorrhagic fever caused by a novel Bunyavirus
559 in China: pathogenesis and correlates of fatal outcome. Clin Infect Dis 54:527-33.
560 7. Yun SM, Park SJ, Kim YI, Park SW, Yu MA, Kwon HI, Kim EH, Yu KM, Jeong HW, Ryou J, Lee WJ,
561 Jee Y, Lee JY, Choi YK. 2020. Genetic and pathogenic diversity of severe fever with
562 thrombocytopenia syndrome virus (SFTSV) in South Korea. JCI Insight 5.
563 8. Li J, Li S, Yang L, Cao P, Lu J. 2021. Severe fever with thrombocytopenia syndrome virus: a highly
564 lethal bunyavirus. Crit Rev Microbiol 47:112-125.
565 9. Anonymous. 2018. Annual review of diseases prioritized under the Research and Development
566 Blueprint, Informal consultation. World Health Organization,
567 https://www.who.int/docs/default-source/blue-print/2018-annual-review-of-diseases-
568 prioritized-under-the-research-and-development-blueprint.pdf?sfvrsn=4c22e36_2.
569 10. Diseases NIoAaI. 2018. NIAID Emerging Infectious Diseases/Pathogens - Category C. Diseases
570 BaEI,
571 11. Plegge T, Hofmann-Winkler H, Spiegel M, Pöhlmann S. 2016. Evidence that Processing of the
572 Severe Fever with Thrombocytopenia Syndrome Virus Gn/Gc Polyprotein Is Critical for Viral
573 Infectivity and Requires an Internal Gc Signal Peptide. PLoS One 11:e0166013.
574 12. Halldorsson S, Behrens AJ, Harlos K, Huiskonen JT, Elliott RM, Crispin M, Brennan B, Bowden TA.
575 2016. Structure of a phleboviral envelope glycoprotein reveals a consolidated model of
576 membrane fusion. Proc Natl Acad Sci U S A 113:7154-9.
577 13. Guo X, Zhang L, Zhang W, Chi Y, Zeng X, Li X, Qi X, Jin Q, Zhang X, Huang M, Wang H, Chen Y, Bao
578 C, Hu J, Liang S, Bao L, Wu T, Zhou M, Jiao Y. 2013. Human antibody neutralizes severe Fever
579 with thrombocytopenia syndrome virus, an emerging hemorrhagic Fever virus. Clin Vaccine
580 Immunol 20:1426-32.
581 14. Kim KH, Kim J, Ko M, Chun JY, Kim H, Kim S, Min JY, Park WB, Oh MD, Chung J. 2019. An anti-Gn
582 glycoprotein antibody from a convalescent patient potently inhibits the infection of severe fever
583 with thrombocytopenia syndrome virus. PLoS Pathog 15:e1007375.

584 15. Wu Y, Zhu Y, Gao F, Jiao Y, Oladejo BO, Chai Y, Bi Y, Lu S, Dong M, Zhang C, Huang G, Wong G, Li
585 N, Zhang Y, Li Y, Feng WH, Shi Y, Liang M, Zhang R, Qi J, Gao GF. 2017. Structures of phlebovirus
586 glycoprotein Gn and identification of a neutralizing antibody epitope. Proc Natl Acad Sci U S A
587 114:E7564-E7573.
588 16. Kwak J-E, Kim Y-I, Park S-J, Yu M-A, Kwon H-I, Eo S, Kim T-S, Seok J, Choi W-S, Jeong JH, Lee H,
589 Cho Y, Kwon JA, Jeong M, Maslow JN, Kim Y-E, Jeon H, Kim KK, Shin E-C, Song M-S, Jung JU, Choi
590 YK, Park S-H. 2019. Development of a SFTSV DNA vaccine that confers complete protection
591 against lethal infection in ferrets. Nature Communications 10:3836.
592 17. Park SJ, Kim YI, Park A, Kwon HI, Kim EH, Si YJ, Song MS, Lee CH, Jung K, Shin WJ, Zeng J, Choi Y,
593 Jung JU, Choi YK. 2019. Ferret animal model of severe fever with thrombocytopenia syndrome
594 phlebovirus for human lethal infection and pathogenesis. Nat Microbiol 4:438-446.
595 18. Choi Y, Jiang Z, Shin WJ, Jung JU. 2020. Severe Fever with Thrombocytopenia Syndrome Virus
596 NSs Interacts with TRIM21 To Activate the p62-Keap1-Nrf2 Pathway. J Virol 94.
597 19. Zimmermann P, Curtis N. 2019. Factors That Influence the Immune Response to Vaccination.
598 Clinical Microbiology Reviews 32:e00084-18.
599 20. Pollard AJ, Bijker EM. 2021. A guide to vaccinology: from basic principles to new developments.
600 Nature Reviews Immunology 21:83-100.
601 21. Gause KT, Wheatley AK, Cui J, Yan Y, Kent SJ, Caruso F. 2017. Immunological Principles Guiding
602 the Rational Design of Particles for Vaccine Delivery. ACS Nano 11:54-68.
603 22. Porter CJH, Trevaskis NL. 2020. Targeting immune cells within lymph nodes. Nature
604 Nanotechnology 15:423-425.
605 23. Kelly HG, Tan HX, Juno JA, Esterbauer R, Ju Y, Jiang W, Wimmer VC, Duckworth BC, Groom JR,
606 Caruso F, Kanekiyo M, Kent SJ, Wheatley AK. 2020. Self-assembling influenza nanoparticle
607 vaccines drive extended germinal center activity and memory B cell maturation. JCI Insight 5.
608 24. Link A, Zabel F, Schnetzler Y, Titz A, Brombacher F, Bachmann MF. 2012. Innate immunity
609 mediates follicular transport of particulate but not soluble protein antigen. J Immunol 188:3724-
610 33.
611 25. Kim YI, Kim D, Yu KM, Seo HD, Lee SA, Casel MAB, Jang SG, Kim S, Jung W, Lai CJ, Choi YK, Jung
612 JU. 2021. Development of Spike Receptor-Binding Domain Nanoparticles as a Vaccine Candidate
613 against SARS-CoV-2 Infection in Ferrets. mBio 12.
614 26. Kanekiyo M, Bu W, Joyce MG, Meng G, Whittle JR, Baxa U, Yamamoto T, Narpala S, Todd JP, Rao
615 SS, McDermott AB, Koup RA, Rossmann MG, Mascola JR, Graham BS, Cohen JI, Nabel GJ. 2015.
616 Rational Design of an Epstein-Barr Virus Vaccine Targeting the Receptor-Binding Site. Cell
617 162:1090-100.
618 27. Kanekiyo M, Wei CJ, Yassine HM, McTamney PM, Boyington JC, Whittle JR, Rao SS, Kong WP,
619 Wang L, Nabel GJ. 2013. Self-assembling influenza nanoparticle vaccines elicit broadly
620 neutralizing H1N1 antibodies. Nature 499:102-6.
621 28. Kim YS, Son A, Kim J, Kwon SB, Kim MH, Kim P, Kim J, Byun YH, Sung J, Lee J, Yu JE, Park C, Kim YS,
622 Cho NH, Chang J, Seong BL. 2018. Chaperna-Mediated Assembly of Ferritin-Based Middle East
623 Respiratory Syndrome-Coronavirus Nanoparticles. Front Immunol 9:1093.
624 29. Domnich A, Arata L, Amicizia D, Puig-Barbera J, Gasparini R, Panatto D. 2017. Effectiveness of
625 MF59-adjuvanted seasonal influenza vaccine in the elderly: A systematic review and meta-
626 analysis. Vaccine 35:513-520.
627 30. Podda A, Del Giudice G. 2003. MF59-adjuvanted vaccines: increased immunogenicity with an
628 optimal safety profile. Expert Review of Vaccines 2:197-204.
629 31. Pellegrini M, Nicolay U, Lindert K, Groth N, Della Cioppa G. 2009. MF59-adjuvanted versus non-
630 adjuvanted influenza vaccines: integrated analysis from a large safety database. Vaccine
631 27:6959-65.

632 32. Tsai TF. 2013. Fluad(R)-MF59(R)-Adjuvanted Influenza Vaccine in Older Adults. Infect Chemother
633 45:159-74.
634 33. Maini MK, Pallett LJ. 2018. Defective T-cell immunity in hepatitis B virus infection: why
635 therapeutic vaccination needs a helping hand. Lancet Gastroenterol Hepatol 3:192-202.
636 34. Thimme R. 2021. T cell immunity to hepatitis C virus: Lessons for a prophylactic vaccine. J
637 Hepatol 74:220-229.
638 35. Sadoff J, Le Gars M, Shukarev G, Heerwegh D, Truyers C, de Groot AM, Stoop J, Tete S, Van
639 Damme W, Leroux-Roels I, Berghmans P-J, Kimmel M, Van Damme P, de Hoon J, Smith W,
640 Stephenson KE, De Rosa SC, Cohen KW, McElrath MJ, Cormier E, Scheper G, Barouch DH,
641 Hendriks J, Struyf F, Douoguih M, Van Hoof J, Schuitemaker H. 2021. Interim Results of a Phase
642 1–2a Trial of Ad26.COV2.S Covid-19 Vaccine. New England Journal of Medicine 384:1824-1835.
643 36. (CDC) CfDCaP. 2023. What you need to know about Asian longhorned ticks - a new tick in the
644 United States.
645 37. Zhang X, Zhao C, Cheng C, Zhang G, Yu T, Lawrence K, Li H, Sun J, Yang Z, Ye L, Chu H, Wang Y,
646 Han X, Jia Y, Fan S, Kanuka H, Tanaka T, Jenkins C, Gedye K, Chandra S, Price DC, Liu Q, Choi YK,
647 Zhan X, Zhang Z, Zheng A. 2022. Rapid Spread of Severe Fever with Thrombocytopenia
648 Syndrome Virus by Parthenogenetic Asian Longhorned Ticks. Emerg Infect Dis 28:363-372.
649 38. Yun SM, Lee WG, Ryou J, Yang SC, Park SW, Roh JY, Lee YJ, Park C, Han MG. 2014. Severe fever
650 with thrombocytopenia syndrome virus in ticks collected from humans, South Korea, 2013.
651 Emerg Infect Dis 20:1358-61.
652 39. Kimura M, Egawa K, Ozawa T, Kishi H, Shimojima M, Taniguchi S, Fukushi S, Fujii H, Yamada H,
653 Tan L, Sano K, Katano H, Suzuki T, Morikawa S, Saijo M, Tani H. 2021. Characterization of
654 pseudotyped vesicular stomatitis virus bearing the heartland virus envelope glycoprotein.
655 Virology 556:124-132.
656 40. Lam TT, Liu W, Bowden TA, Cui N, Zhuang L, Liu K, Zhang YY, Cao WC, Pybus OG. 2013.
657 Evolutionary and molecular analysis of the emergent severe fever with thrombocytopenia
658 syndrome virus. Epidemics 5:1-10.
659 41. Xia T, Wu X, Hong E, Jung K, Lai C-J, Kwak M-J, Seo H, Kim S, Jiang Z, Cha I, Jung JU. 2023.
660 Glucosylceramide is essential for Heartland and Dabie bandavirus glycoprotein-induced
661 membrane fusion. PLOS Pathogens 19:e1011232.
662 42. Yoshikawa T, Shimojima M, Fukushi S, Tani H, Fukuma A, Taniguchi S, Singh H, Suda Y, Shirabe K,
663 Toda S, Shimazu Y, Nomachi T, Gokuden M, Morimitsu T, Ando K, Yoshikawa A, Kan M, Uramoto
664 M, Osako H, Kida K, Takimoto H, Kitamoto H, Terasoma F, Honda A, Maeda K, Takahashi T,
665 Yamagishi T, Oishi K, Morikawa S, Saijo M. 2015. Phylogenetic and Geographic Relationships of
666 Severe Fever With Thrombocytopenia Syndrome Virus in China, South Korea, and Japan. J Infect
667 Dis 212:889-98.
668 43. Li A, Liu L, Wu W, Liu Y, Huang X, Li C, Liu D, Li J, Wang S, Li D, Liang M. 2021. Molecular
669 evolution and genetic diversity analysis of SFTS virus based on next-generation sequencing.
670 Biosafety and Health 3:105-115.
671 44. Yun SM, Park SJ, Park SW, Choi W, Jeong HW, Choi YK, Lee WJ. 2017. Molecular genomic
672 characterization of tick- and human-derived severe fever with thrombocytopenia syndrome
673 virus isolates from South Korea. PLoS Negl Trop Dis 11:e0005893.
674 45. Jia Z, Wu X, Wang L, Li X, Dai X, Liang M, Cao S, Kong Y, Liu J, Li Y, Wang J. 2017. Identification of
675 a candidate standard strain of severe fever with thrombocytopenia syndrome virus for vaccine
676 quality control in China using a cross-neutralization assay. Biologicals 46:92-98.
677 46. Kwang-Min Yu S-JP, Min-Ah Yu, Young-Il Kim, Younho Choi, Jae U. Jung, Benjamin Brennan,
678 Young Ki Choi. 2019. Cross-genotype protection of live-attenuated vaccine candidate for severe
679 fever with thrombocytopenia syndrome virus in a ferret model. PNAS 116:26900-26908.

680 47. Mastronarde DN. 2005. Automated electron microscope tomography using robust prediction of
681 specimen movements. J Struct Biol 152:36-51.
682 48. Punjani A, Rubinstein JL, Fleet DJ, Brubaker MA. 2017. cryoSPARC: algorithms for rapid
683 unsupervised cryo-EM structure determination. Nat Methods 14:290-296.
684 49. Yu KM, Yu MA, Park SJ, Kim YI, Robles NJ, Kwon HI, Kim EH, Si YJ, Nguyen HD, Choi YK. 2018.
685 Seroprevalence and genetic characterization of severe fever with thrombocytopenia syndrome
686 virus in domestic goats in South Korea. Ticks Tick Borne Dis 9:1202-1206.

687

688

689 **Figure Legends**

690 **Fig 1. Molecular design and biochemical and antigenic characterization of ferritin**
691 **nanoparticles (FT) and DBV Gn Head-ferritin (GnH-FT) nanoparticles**

692 (A) Schematic representation of GnH-FT based on previously solved structures and domains of
693 DBV Gn and Gc. The construct was transfected to HEK293T cells to collect the cell supernatant
694 at 72 hours after transfection for purification. (SP: signal peptide, TM: transmembrane domain)
695 (B, C) Size exclusion chromatograms to purify FT (B) and GnH-FT (C) using Superdex 200.
696 Increase 10/300 GL and Superose6 Increase 10/300 GL columns, respectively, on Bio-Rad
697 NGC chromatography system. Fractions corresponding to the colored arrows were separately
698 collected for further analyses.
699 (D, E) Fractions from size exclusion chromatograms of FT and GnH-FT were further analyzed
700 by gradient (7% - 20%) SDS-PAGE and Coomassie Brilliant blue staining. Fractions
701 corresponding to the black and red arrows from FT and GnH-FT purifications were loaded to
702 SDS-PAGE gel without boiling ("NB") and with boiling ("B") to characterize head-mediated
703 disassembly of the 24-mer nanoparticle. Intact FT nanoparticle and GnH-FT nanoparticle each
704 has expected molecular weight of approximately 432 kDa and 1,560 kDa. Dissembled FT and
705 GnH-FT monomer each has expected molecular weight of 18 kDa and 65 kDa.
706 (F) Western-blot analysis of different fractions collected from GnH-FT size exclusion
707 chromatogram. In house-generated mouse monoclonal antibody recognizing DBV Gn Head
708 region was used to detect GnH-FT subunit monomers.
709

710 **Fig 2. Prediction and observed structures of FT and GnH-FT nanoparticles**

711 (A, B) Computer-assisted 3D model of the FT nanoparticles (A) and GnH-FT nanoparticles (B)
712 based on previously solved structures of DBV Gn (PDB: 5Y11) and FT nanoparticles (PDB:
713 3EGM).
714 (C, D) Cryo-electron microscopy (cryo-EM) of FT (C) and GnH-FT (D) nanoparticles.
715 (E, F) Representative 2D class averages of FT (E) and GnH-FT (F). The white halo surrounding
716 the FT nanoparticle core in (F) is attributable to the highly flexible linker and DBV Gn head
717 domain.
718

719 **Fig 3. Immunization with GnH-FT elicits humoral and cellular immunity *in vivo***

720 (A) Timeline for mouse immunization and blood collection. Six BALB/c mice per antigen group
721 were intramuscularly immunized at hind leg with 3.3μg of FT or 1μg, 5μg, or 10μg of GnH-FT.
722 3.3μg of FT is equimolar to 10μg of GnH-FT.

723 (B) Reciprocal IgG titer measured by ELISA using purified GnH-10His protein coated. Sera from
724 blood samples collected at weeks 0, 2, 3, 5, 6, and 8 were used to quantify total IgG recognizing
725 DBV Gn Head. Endpoint titer values are presented in $\log_{10}$ values. The asterisks represent
726 statistical significance of endpoint titer between mice immunized with GnH-FT and FT evaluated
727 with one-way ANOVA with Dunnett multiple comparison test.
728 (C) Neutralizing antibody titer measured by luciferase assay using rVSV-DBV G carrying
729 luciferase gene. Sera from blood samples collected at weeks 0, 2, 5, and 8 were used to
730 quantify reciprocal IC_{50} titer to represent induction of neutralizing antibody upon immunization
731 with different antigens. One-way ANOVA with Dunnett multiple comparison test was performed.
732 (D) ELISpot assays were performed to detect DBV Gn Head-specific T cells secreting IFN-γ by
733 *ex vivo* stimulation of whole splenocytes with pool of overlapping peptides (OLP). Data
734 represents the number of spot-forming units (SFUs) per 1 million splenocytes. One-way ANOVA
735 with Dunnett multiple comparison test was used to evaluate statistical significance.
736 (E) Intracellular cytokine staining assay was performed to test for activity of cellular immunity
737 induced upon immunization with the antigens. Splenocytes were stimulated *ex vivo* as for
738 ELISpot assay, treated with protein transport inhibitor, then stained for anti-TNF-α antibodies or
739 IL-2 antibodies. Two-tailed, unpaired t-test was performed to evaluate statistical significance.
740 *P < 0.05, **P < 0.01, ***P < 0.001 and ****P < 0.00001.
741
742 **Fig 4. Aged ferrets form humoral immunity upon immunization with GnH-FT**
743 (A) Timeline for aged ferret immunization, lethal DBV challenge, and organ harvest. Based on
744 the effective induction of humoral and cellular immunity in mouse model, aged ferrets were
745 immunized with total three doses of 15μg GnH-FT or FT. Each antigen group had 12 ferrets.
746 Aged ferrets were challenged with $10^{7.6}$ $TCID_{50}$/mL of DBV for infection with lethal dose at 2
747 weeks after the last booster immunization, then monitored for clinical symptoms of SFTS. At 2,
748 4, and 6 days post the challenge, three ferrets per antigen group were sacrificed to harvest
749 serum, spleen, liver, and kidney for organ virus titration to test for acceleration in viral clearance.
750 (B) Reciprocal IgG titer measured by ELISA using blood samples collected at days -42, -28, -14
751 and 0 to characterize humoral immunity induced by immunization with FT or GnH-FT. Optical
752 density (OD) was measured with a spectrometer (VarioSkan, Thermo) at detection wavelength
753 of 450nm.The asterisks represent statistical significance of OD measurements from ferrets
754 immunized with GnH-FT to ferrets immunized with FT evaluated with one-way ANOVA with
755 Dunnett multiple comparison test.

(C) Neutralizing antibody response to DBV elicited by immunization with FT or GnH-FT was characterized as $FRNT_{50}$ from blood samples collected at days -28, -14, and 0 to represent time points of 2 weeks after the 1st, 2nd, and 3rd vaccination. The asterisks represent statistical significance of $FRNT_{50}$ from ferrets immunized with GnH-FT to ferrets immunized with FT evaluated with one-way ANOVA with Dunnett multiple comparison test.

*P < 0.05, **P < 0.01, ***P < 0.001 and ****P < 0.00001.

Fig 5. Protective immunity elicited by GnH-FT nanoparticle immunization against lethal DBV challenge in aged ferrets

(A, B, C) Body weight (A), survival curve (B) and temperature (C) of the aged ferrets were observed for 14 days from the lethal challenge. Body weight and temperature are presented as mean ± SEM and statistical significance was analyzed by one-way ANOVA with Dunnett multiple comparison test. Statistical significance of survival across the antigens was analyzed with 2-tailed Mantel-Cox method.

(D, E) White blood cell (WBC, D) and platelet (E) counts were measured from blood samples collected for 14 days after the lethal challenge. Data are presented as box plots with the upper (75%) and lower (25%) quartiles, the horizontal line (median) and whiskers (maximum and minimum). Statistical significance across the antigens was evaluated by a two-tailed unpaired t-test.

*P < 0.05, **P < 0.01, ***P < 0.001 and ****P < 0.00001.

Fig 6. Viral titration from serum, spleen, liver, and kidney

Organs were harvested at days 2, 4, and 6 from three animals at each time point. DBV titer values from serum (A), spleen (B), liver (C), and kidney (D) were measured with real-time PCR. Data are shown as mean ± SEM. The asterisks indicate statistical significance compared between ferrets immunized with FT nanoparticle and GnH-FT nanoparticle from the two-tailed, unpaired t-test.

*P < 0.05, **P < 0.01, ***P < 0.001 and ****P < 0.00001.

Figure 1. Molecular design of DBV GnH-ferritin nanoparticles

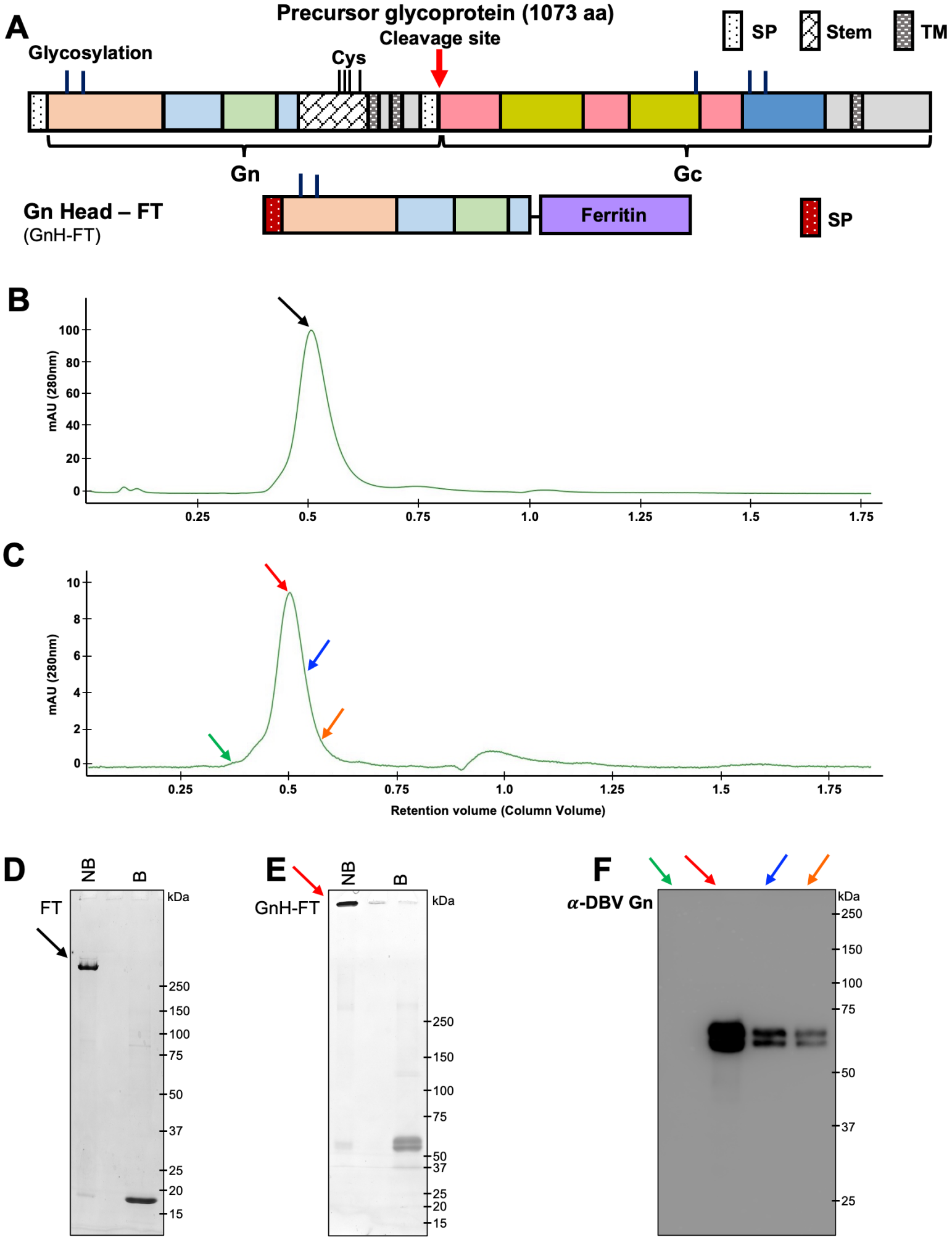

Figure 2. Structural analysis of FT and GnH-FT nanoparticle

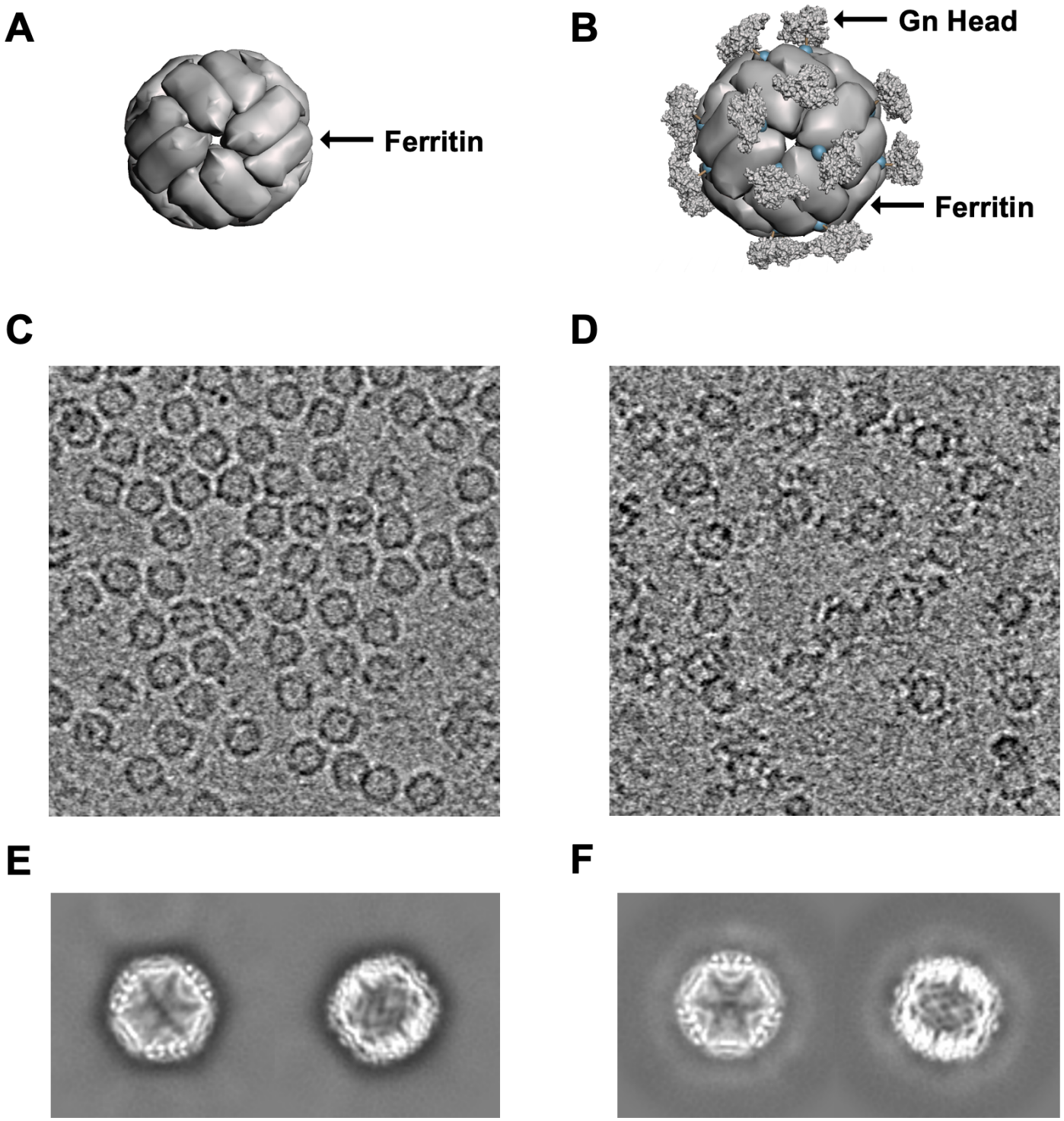

Figure 3. Mice immunized with GnH-FT develops humoral and cellular immunity against DBV

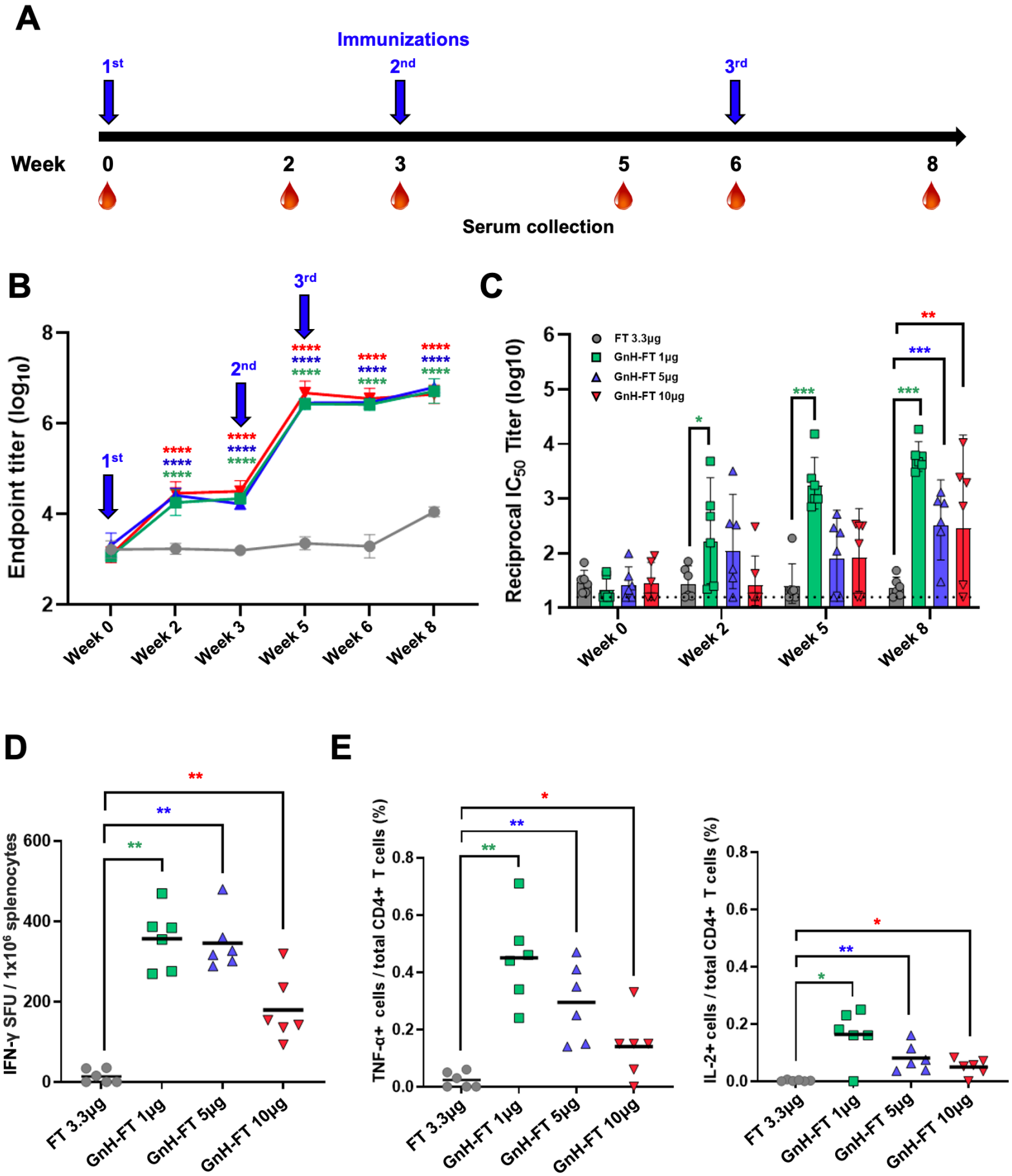

* P <0.05, ** P<0.01, *** P<0.001, and **** P<0.00001

Figure 4. Aged ferrets immunized with GnH-FT develops immunity against DBV

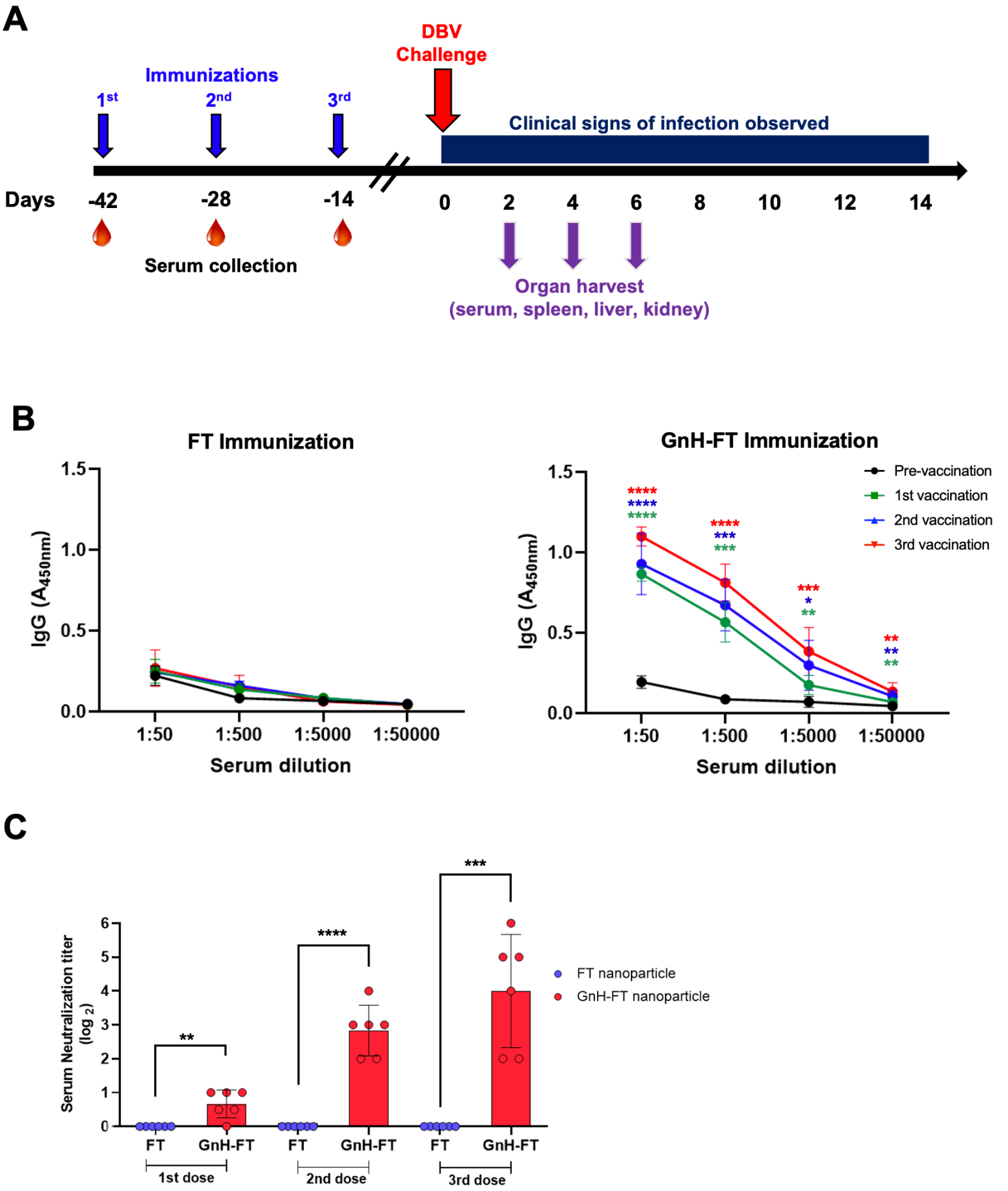

** P <0.05, ** P<0.01, *** P<0.001, and **** P<0.00001*

Figure 5. Aged ferrets immunized with GnH-FT are fully protected from lethal DBV challenge

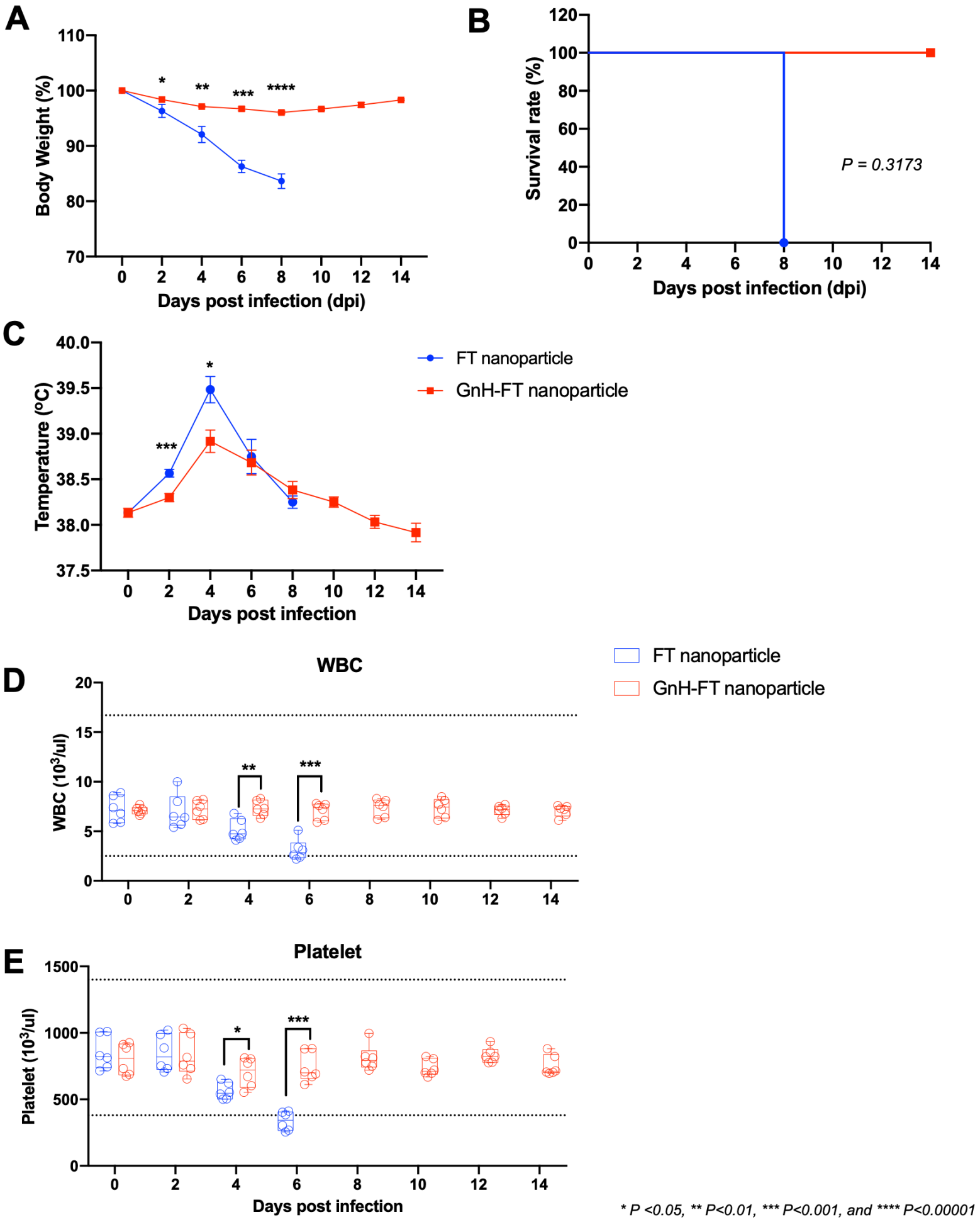

* P <0.05, ** P<0.01, *** P<0.001, and **** P<0.00001

Figure 6. Aged ferrets immunized with GnH-FT suppress viral replication and rapidly clears virus from lethal DBV challenge

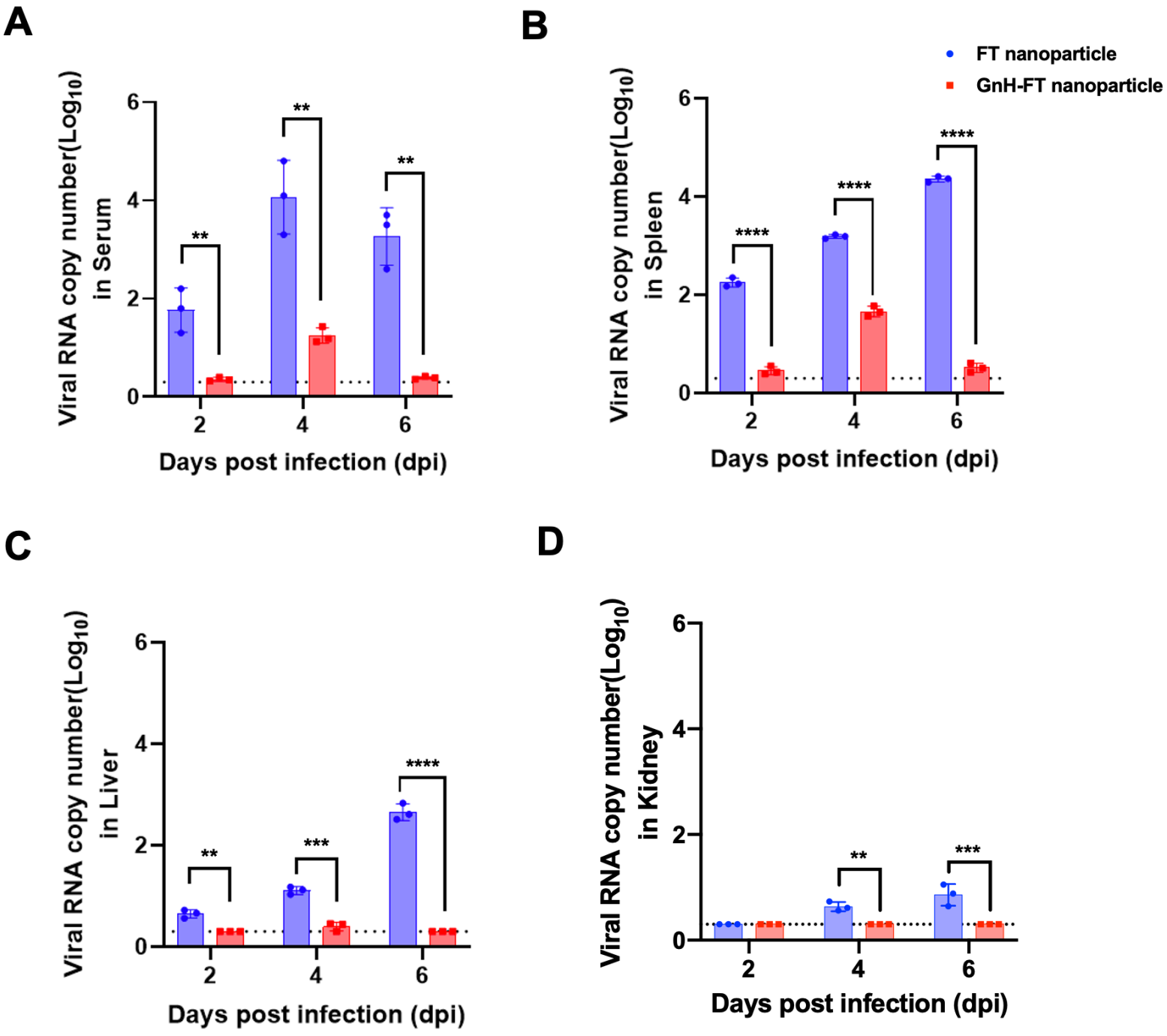

** P <0.05, ** P<0.01, *** P<0.001, and **** P<0.00001*